Nonlinear Transmission Performance in Delay-Managed Few-Mode Fiber Links with Intermediate Coupling

Filipe M. Ferreira, Christian S. Costa, Naoise Mac Suibhne, Stylianos Sygletos, Andrew D. Ellis
Aston Institute of Photonic Technologies, Aston University, Birmingham, UK (f.ferreira@aston.ac.uk))

Abstract: Linear equalization performance for delay-managed few-mode links in the nonlinear regime with intermediate linear coupling is studied for the first time. Existing fibers can allow similar performance per mode to that of uncoupled single-mode propagation.
OCIS codes: (060.0060) Fiber optics and optical communications; (060.4370) Nonlinear optics, fibers.

1. Introduction

Mode-division multiplexing over few-mode fibers (FMFs) is emerging as a potential solution to overcome the impeding installed capacity exhaustion of current single-mode fibers (SMFs). Nevertheless, in order to access FMFs full capacity additional impairments have to be overcome, namely: linear mode coupling [1,2] (XT), differential mode delay [1,2] (DMD), and inter-mode nonlinear effects (IM-NL) [3,4]. In the linear regime, the transmission performance is either limited by noise or limited by the group delay (GD) spread induced by the interplay between XT and DMD [2]. GD spread does not impose a fundamental limitation as it can be successfully compensated through multiple-input-multiple-output (MIMO) equalization provided that the channel memory is shorter than the equalizer memory. Although, in the nonlinear regime, performance degradation can be dominated by IM-NL interactions in particular for low DMD and XT values [5,6]. However whilst IM-NL interactions have been experimentally measured [3], numerically modelled and characterized [7-10], to the best of our knowledge MIMO equalization performance has not been characterized for DMD managed links operating in nonlinear regime with intermediate linear coupling.

In this paper, we evaluate MIMO equalization for 6-mode transmission of dual-polarization (DP) quadrature phase-shift keyed (QPSK) signals over DMD managed spans operating in the nonlinear regime with intermediate coupling.

2. Transmission Link Modelling

Transmitter and receiver: Twelve 28 GBd QPSK signals are transmitted, one per orthogonal polarization of a 6-mode FMF (LP_{01}, LP_{02}, LP_{11a}, LP_{11b}, LP_{21a}, LP_{21b}) yielding a total bit rate of 672 Gb/s per wavelength. Together with the information data, a preamble is transmitted consisting of constant amplitude zero autocorrelation (CAZAC) sequences, used for time synchronization and channel estimation. Root raised cosine filters with a roll-off factor of 0.001 are used for pulse shaping. After homodyne detection, the baseband electrical signals are sampled at 56 GS/s, yielding 12 digital signals with 2 samples/symbol. Chromatic dispersion is compensated in the frequency domain using the chromatic dispersion averaged over the modes. Coarse time synchronization is performed using the Schmidl & Cox autocorrelation metric. Subsequently, fine-time synchronization and channel impulse response (CIR) estimation is performed by cross-correlating with the training CAZAC sequences. The 12×12 CIR estimations are converted into the frequency domain. The MIMO frequency domain equalizer is calculated by inverting the channel matrix, and, finally, the total Q-factor for each received signal is calculated.

Nonlinear Fiber Model: The link performance was calculated by numerically solving the coupled nonlinear Schrödinger equation, which can be written for a given mode *s* and polarization *l*, at reference frequency ω_0 as [7-10]:

$$\left(\partial_z + \beta_{sl}^{(1)}\partial_t - \mathrm{j}\frac{\beta_{sl}^{(2)}}{2}\partial_t^2 \ldots\right)A_{sl} = -\mathrm{j}\sum_{pi,qj,rk}\xi_{ijkl}\,\gamma_{pqrs}A_{pi}A_{qj}A_{rk}^{*}e^{-\mathrm{j}\Delta\beta_{pi,qj,rk,sl}z} - \mathrm{j}\sum_{pi}A_{pi}\,C_{sl,pi}e^{\mathrm{j}\left(\beta_{sl}^{(0)}-\beta_{pi}^{(0)}\right)z} \quad (1)$$

where $\{p, q, r, s\}$ are mode indices; $\{i, j, k, l\}$ are polarization indices; * stands for complex conjugate; A_{sl} is the slowly varying envelope of wave *sl*; $\beta_{sl}^{(m)}$ is the value of the m^{th} angular frequency derivative of the propagation constant $\beta_{sl}(\omega)$ at ω_0; $\Delta\beta_{pi,qj,rk,sl} = \beta_{pi}^{(0)} + \beta_{qj}^{(0)} - \beta_{rk}^{(0)} - \beta_{sl}^{(0)}$ is the phase mismatch between waves $(pi,\ qj,\ rk,\ sl)$; $\xi_{ijkl} = \delta_{il}\delta_{jl}\delta_{kl} + 2/3\,\delta_{il}\delta_{jl_\perp}\delta_{kl_\perp} + 1/3\,\delta_{il_\perp}\delta_{jl_\perp}\delta_{kl}$ groups the independent polarization combinations using the Kronecker delta function δ_{il}; γ_{pqrs} is the inter-mode nonlinear coefficient between modes (p, q, r, s); the Kerr coefficient, approximately equal to $2.6\cdot10^{-20}$ m^2/W; $C_{pi,sl}$ is the linear mode coupling coefficient between mode *pi* and mode *sl*. The 1st term on the right-hand side of (1) is responsible for all the NL effects taking place between the wave *sl* and the all the other 2 × 6 waves (including itself), this is, it includes: self-phase modulation, cross-phase modulation, four-wave mixing, and inter-mode counterparts [3]. The 2nd term on right-hand side of (1) is responsible for the linear mode coupling [8].

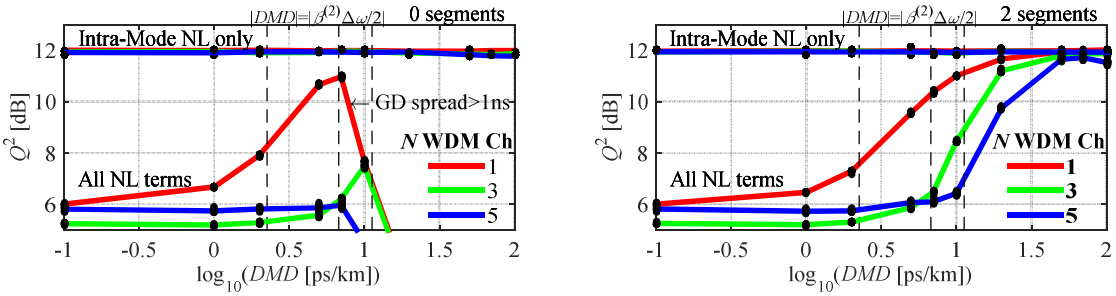

Fig. 1. Q^2 [dB] of the LP_{01} center channel in the absence of mode coupling as a function of *DMD*, for: (a) 0 and (b) 2 segments.

Linear Mode Coupling Model: The model considers multiple fiber sections with a random displacement of the core center position (along radial and azimuthal coordinates) [8]. In this way, each section has constant coupling coefficients allowing for a semi-analytical solution of the 2nd term on right-hand side of (1) that were used to modify the split-step Fourier method for few-mode propagation including mode coupling as in [8]. Finally, the mode coupling strength is set by varying the fiber displacement as show in [11]. The mode coupling strength (*XT*) is quantified as $XT_p = \sum_{q \neq p} P_q / P_p$ where P_p is the power of mode *p*, after a given segment under test, when only mode *p* was launched. The *XT* value of fabricated FMFs range from -50 dB/100m to -40 dB/100m for step-index and graded-index profiles [12,13], going up to -28 dB/100m for coupled multi-core fibers [14] and -7 dB/100m for ring-core fibers [15].

Delay compensation segment: The first fiber considered has a graded-index core and a cladding trench with a refractive index relative difference of 4.5×10^{-3} and a radius of 12.83 μm, optimized in [16] for different values of low DMD. The uncoupled GD vector is (0, 8, 13, 14, 17, 18) ps/km for (LP_{01}, LP_{02}, LP_{11a}, LP_{11b}, LP_{21a}, LP_{21b}), respectively, *DMD* is equal to 18 ps/km. The remaining characteristics are available in [16]. Finally, we anticipate that a resonant DMD map would represent a worst case condition, and so for simplicity the second fiber is assumed to be identical to the first, but with the opposite values of *DMD* per fiber. Finally, different *DMD* values were obtained by scaling the GD vector allowing for an objective assessment of the linear equalizer performance as other fiber characteristics are kept.

3. Results

In this section, we study MIMO equalization performance considering the transmission of an optical super-channel consisting of 5 channels 28 Gbaud DP-QPSK per mode (spaced of 28.1 GHz), giving a total bit rate of 3.3 Tb/s, over 100 km. The performance is calculated for a range of different: *XT* values (-50 dB/100m to 0 dB/100m), *DMD* values (0.1 to 1000 ps/km), and number of DMD compensation segments (0 to 10, 0 means no DMD compensation, 10 means 10 pairs of DMD-positive-DMD-negative fibers). The power per channel is set to 11.7 dBm so the system is operating in the nonlinear regime, and the Q-factor of the LP_{01} center channel is equal to 12 dB. The length of the training CAZAC sequences were set to compensate for a maximum GD spread of 1 ns.

Fig. 1 shows the Q^2 [dB] of the LP_{01} center channel in the absence of mode coupling as a function of *DMD*, considering {1, 3, 5} WDM channels, for: (a) 0 and (b) 2 segments. Moreover, there are two sets of results: one obtained considering all NL terms in (1) and another considering only the intra-mode NL terms, this is, uncoupled single-mode propagation for performance reference (in the latter case arbitrarily long CAZAC sequences are used). In Fig. 1 (a), obtained in the absence of DMD management, it can be seen that by increasing *DMD*, Q^2 starts approaching that of uncoupled single-mode propagation, however, around *DMD* = 10 ps/km, Q^2 drops as the maximum GD spread is reached. In Fig. 1 (b), obtained considering 2 segments for DMD compensation, it can be seen that by increasing *DMD*, Q^2 eventually equals that of uncoupled single-mode propagation. Note that Q^2 starts increasing when *DMD* is higher than the walk-off induced by chromatic dispersion ($|\beta_2 \Delta\omega_{WDM}/2|$) as indicated by the vertical dashed lines. However, when mode coupling is present the DMD compensation will not be so effective requiring the usage of a higher number of segments to avoid hitting the maximum GD spread allowed, which by its turn will increase the NL penalty given the enhancement of the DMD map resonance, a tradeoff assessed in the following.

Fig. 2 shows a contour plot of the Q^2 [dB] of the LP_{01} center channel normalized to the Q^2 of uncoupled single-mode propagation, as a function of *XT* and *DMD*. Four DMD managed scenarios are shown: (a) non-DMD-managed, (b) 2, (c) 5 and (d) 10 segments. In Fig. 2, there are two highlighted areas where $Q^2 < 6.7$ dB (below FEC threshold): one where the GD spread is longer than the training CAZAC sequences length (validated by considering linear propagation), and one for which the IM-NL penalty is equal or higher than the intra-mode NL penalty. Regarding the $Q^2 < 6.7$ dB area due to GD spread, it can be seen that the area shrinks with increasing number of segments, as DMD compensation gets more effective, this is, higher values of *XT* and *DMD* can be tolerated given shorter compensation lengths. However, the $Q^2 < 6.7$ dB area given the IM-NL penalty does not vary significantly with the number segments (some expansion is visible at contours bottom half), as previously found in [5,6].

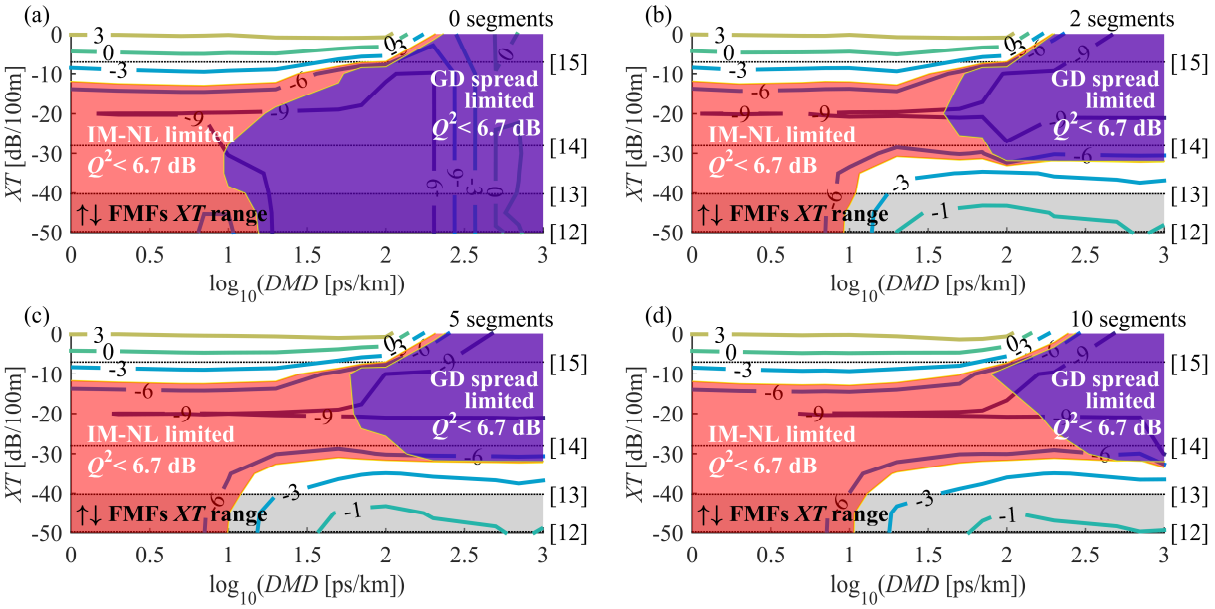

Fig. 2. Contour plots of the Q^2 [dB] of the center channel in the LP_{01} normalized to that of uncoupled single-mode propagation, as a function of *XT* and *DMD*. Four DMD maps are considered: (a) non-GD-managed, (b) 2, (c) 5 and (d) 10 segments.

Furthermore, at Fig. 2 outside the Q^2 <6.7 dB areas, it can be seen that partial suppression of the IM-NL penalty can be obtained for *DMD* > 100 ps/km and *XT* < -30 dB/100m when considering DMD-managed spans, unlike non-DMD-managed spans for which the maximum GD spread is hit before a significant suppression can be observed. More importantly, for *DMD* ≈ 150 ps/km and *XT* < -45 dB/100m, an operation regime that can be achieved using existing FMFs, the Q^2 difference between coupled few-mode propagation and uncoupled single-mode propagation is under 1 dB (where few-mode propagation Q^2 is lower). Finally, from Fig. 2, it can be seen that suppression of the total NL penalty below that of uncoupled single-mode propagation can be obtained for *XT* > -5 dB/100m and *DMD* < 150 ps/km.

4. Conclusions

MIMO equalization performance in delay-compensated few-mode links operating simultaneously in the nonlinear regime and intermediate coupling regime is studied for the first time. The results shown that existing FMFs can allow a similar performance (per mode) to that of uncoupled single-mode propagation (Q^2 difference is under 1 dB). Furthermore, better performance per mode in few-mode propagation can be achieved for strong mode coupling (*XT* > -5 dB/100m) and moderate *DMD* values (< 150 ps/km).

This work has been partially supported by the European Union (Grants 619732-INSPACE, 654809-HSPACE, 659950-INVENTION, and 627545-SOLAS), and by the EPSRC (Grant EP/L000091/1-PEACE).

5. References

[1] D. Marcuse, Theory of Dielectric Optical Waveguides, 2nd ed. New York: Academic, 1991.
[2] K. Ho, et al., "Statistics of group delays in multimode fiber with strong mode coupling," J. Lightw. Technol., **29**(21), p 3119, (2011).
[3] R.-J. Essiambre, et al., "Inter-modal nonlinear interactions between well separated channels in spatially-multiplexed fiber transmission," Proc. ECOC, p. Tu.1.C.4, (2012).
[4] F. Poletti, et al., "Description of ultrashort pulse propagation in multimode optical fibers," J. Opt. Soc. Am. B, **25**, p.1645, (2008).
[5] G. Rademacher, et al., "Nonlinear interaction in differential mode delay managed mode-division multiplexed transmission systems," Opt. Express, **23**(1), p. 55, (2015).
[6] F. Ferreira, et al., "Advantages of Strong Mode Coupling for Suppression of Nonlinear Distortion in Few-Mode Fibers," Proc. OFC, p. Tu2E.3, (2016).
[7] C. Antonelli, et al., "Modeling of Nonlinear Propagation in Space-Division Multiplexed Fiber-Optic Transmission," J. Lightw. Technol., **34**(1), p. 36, (2016).
[8] F. Ferreira, et al., "Nonlinear Semi-Analytical Model for Simulation of Few-Mode Fiber Transmission," Photon. Technol. Lett., **24**(4), p.240, (2012).
[9] S. Mumtaz, et al., "Nonlinear Propagation in Multimode and Multicore Fibers: Generalization of the Manakov Equations," J. Lightw. Technol., **31**(3), p.398, (2013).
[10] A. Mecozzi, et al., "Nonlinear propagation in multi-mode fibers in the strong coupling regime," Opt. Express, **20**, p.11673, (2012).
[11] F. Ferreira, et al., "Few-mode fibre group-delays with intermediate coupling," Proc. ECOC, p. Th.1.6.1, (2015).
[12] L. Grüner-Nielsen, et al., "Few Mode Transmission Fiber With Low DGD, Low Mode Coupling, and Low Loss," J. Lightw. Technol., **30**(23), p. 3693, (2012).
[13] T. Mori, et al., "Low DMD Four LP Mode Transmission Fiber for Wide-band WDM-MIMO System," Proc. OFC, p. OTh3K.1, (2013).
[14] R. Ryf, et al., "Space-division multiplexed transmission over 4200-km 3-core microstructured fiber," Proc. OFC, p. PDP5C.2, (2012).
[15] N. Fontaine, et al., "Experimental investigation of crosstalk accumulation in a ring-core fiber," Proc. PSSTMS, p. TuC4.2, (2013).
[16] F. Ferreira, et al., "Design of Few-Mode Fibers With M-modes and Low Differential Mode Delay," J. Lightw. Technol., **32**(3), p. 353, (2014).